

1995/12/366

N95-27787

ULYSSES ORBIT DETERMINATION AT HIGH DECLINATIONS

Timothy P. McElrath and George D. Lewis
Jet Propulsion Laboratory (JPL), California Institute of Technology
Pasadena, California, USA

Abstract

The trajectory of the Ulysses spacecraft caused its geocentric declination to exceed 60° South for over two months during the Fall of 1994, permitting continuous tracking from a single site. During this time, spacecraft operations constraints allowed only Doppler tracking data to be collected, and imposed a high radial acceleration uncertainty on the orbit determination process. The unusual aspects of this situation have motivated a re-examination of the Hamilton-Melbourne results, which have been used before to estimate the information content of Doppler tracking for trajectories closer to the ecliptic. The addition of an acceleration term to this equation is found to significantly increase the declination uncertainty for symmetric passes. In addition, a simple means is described to transform the symmetric results when the tracking pass is non-symmetric. The analytical results are then compared against numerical studies of this tracking geometry and found to be in good agreement for the angular uncertainties. The results of this analysis are applicable to the Near Earth Asteroid Rendezvous (NEAR) mission and to any other missions with high declination trajectories, as well as to missions using short tracking passes and/or one-way Doppler data.

Introduction

The Ulysses mission is a cooperative project of NASA and the European Space Agency (ESA) to send a spacecraft equipped to measure charged and neutral particles, magnetic fields, electro-magnetic waves, and ultraviolet and X-ray emissions over the polar regions of the Sun. Following a Jupiter gravity assist, the Ulysses spacecraft reached South heliographic latitudes in excess of 70 degrees for 132 days starting in June, 1994. Following this time the spacecraft was continuously in view from the Canberra complex of the NASA/JPL Deep Space Network (DSN) from early October to mid-December, and outside of these dates the spacecraft was still in nearly continuous view for some time.

While Ulysses has typically been tracked for ten hours per day, with two-way Doppler and range observations being made simultaneously with telemetry reception, the Sun-spacecraft-Earth geometry during the South solar pass caused the predicted return of solar-induced nutation to the spin-stabilized spacecraft to occur. The method used to control nutation utilized active, unbalanced attitude thruster firings, commanded by the spacecraft in response to conscan measurements of the uplink radio signal. As a result, the Ulysses spacecraft required a continuous, undisturbed uplink during nutation control operations, which extended from August, 1994 through January, 1995. Although the DSN complexes did not have a continuous view throughout this time, an uplink signal and telemetry acquisition for spacecraft monitoring were provided through the use of the ESA tracking station at Kourou, French Guiana. The same situation arises again during the North solar pass, with nutation operations running from late March to October, 1995.

While the nutation control approach used by Ulysses permitted two-way coherent Doppler data to be collected continuously during DSN passes, the ranging tones generated by DSN stations cause enough modulation of the uplink to result in spurious attitude control pulses. Consequently, no ranging data was collected during nutation operations. In addition, the unbalanced nature of the thruster firings meant that up to two cm/sec of delta-V was imparted to the spacecraft per day in the direction toward the Earth. These events were clearly visible in the Doppler data, which has a sensitivity of 0.1 mm/sec under ideal conditions. While the average effect of these events was modelled, based on the average angular rate of the Earth as seen from

the spacecraft, the thruster firings did not occur in an evenly spaced manner. In addition, even if every individual thruster firing could be detected in the tracking or telemetry data (which was not the case), the number of thruster events in a typical three-month data arc was two orders of magnitude more than could be estimated as discrete events using the JPL orbit determination software. Consequently, thruster firing events of more than 1 mm/sec (representing three to four pulses) were dealt with discretely, and the rest of the activity was approximated using the continuous model, and estimated as a series of independent accelerations lasting three hours, with an *a priori* uncertainty of 10^{-10} km/sec².

The trajectory reconstruction requirement for Ulysses is 1000 km (1σ), which would be difficult to meet in the ecliptic under these conditions. However, the high declination of the trajectory would be expected to provide a highly accurate estimate of the geocentric angular position of the spacecraft. The basis for this expectation is the work done by Hamilton and Melbourne in Reference 1. Based on these results, a one-day pass at typical declination and range values for Ulysses would have an expected plane-of-sky uncertainty of about 47 km (or about 140 nanoradians (nrad)), as will be shown in detail later. While this is a highly accurate result, the effect of adding acceleration uncertainty would be expected to increase the plane-of-sky uncertainty. The exact amount of the increase is not immediately obvious, and so the motivation of much of the following analysis is to derive the effect of acceleration uncertainty on the information content of a pass of Doppler data. It should be mentioned that although the Doppler tracking does not directly measure the Earth-spacecraft range, which must also be known to meet the reconstruction requirement, the relative motion of the Earth and the spacecraft over a typical hundred-day data arc is generally sufficient to determine the geocentric range to within an order of magnitude or better of the plane-of-sky position uncertainty.

Analysis

The full derivation of the data equation for a Doppler observation of a distant spacecraft is given in Reference 1, and also revisited with minor corrections by Muellershoen in Reference 2, so only the final result before linearization about the nominal right ascension will be given here. It should be noted, however, that none of the approximations made to reach this result required that the spacecraft declination be small, so this result is as valid for Ulysses as for any spacecraft in the ecliptic, with the only restriction being that the geocentric range be large compared to the radius of the Earth. The topocentric velocity of a distant spacecraft, $\dot{\rho}$, is given by

$$\dot{\rho} \simeq \dot{r} + \omega r_s \cos \delta \sin(\theta - \theta_0) \quad (1)$$

where

- $\dot{\rho}$ = Doppler observable
- \dot{r} = spacecraft's geocentric range-rate
- ω = Earth's rotation rate
- r_s = distance from tracking station to Earth's spin axis
- δ = spacecraft's declination
- θ = tracking station's right ascension
- θ_0 = spacecraft's right ascension

It can almost be proven by inspection that this is the right form, in consideration of the characteristic lengths and the periodicity of the motions involved. Equation (1) can be linearized about an *a priori* relative right ascension, which can then be expressed as a function of time, by re-defining $(\theta - \theta_0)$ as $\omega(t - t_0)$, such that the spacecraft is at the station longitude when $t = 0$. Since ωt_0 is small, we have

$$\begin{aligned} \dot{\rho} &\simeq \dot{r} + \omega r_s \cos \delta \sin \omega t - \omega t_0 \omega r_s \cos \delta \cos \omega t \\ &\simeq a + b \sin \omega t + c \cos \omega t \end{aligned} \quad (2)$$

where

$$\begin{aligned}
a &= \dot{r} \\
b &= \omega r_s \cos \delta \\
c &= -\omega t_0 \omega r_s \cos \delta
\end{aligned}$$

As an aside, it should be noted that representing Doppler data in this form is not unique to navigation at JPL. For instance, radio science processing of Doppler data has been done using equation (2) and the first-order expansion of equation (2) in time, as described in Reference 3. The resulting "six-parameter fit" is fairly efficient in removing all of the dynamics present in a pass of Doppler data for gravity wave detection purposes.

Equation (2) can be extended to handle the effect of a constant radial acceleration by adding a term qt , where q is the acceleration magnitude in the geocentric direction.

$$\dot{\rho} \simeq a + b \sin \omega t + c \cos \omega t + qt \quad (3)$$

The epoch at which the acceleration term does not contribute to the velocity is in the middle of the data arc. Any other placement of the epoch causes a correlation between the radial velocity and the radial acceleration, which adds undesirable complexity to the problem.

Before proceeding to take partials of $\dot{\rho}$ with respect to the four parameters, it is worth noting that b and c may be replaced by new parameters b' and c' such that $\omega t' = \omega t + \phi$ is the new argument of the sine and cosine in equation (3). The angle ϕ then becomes the right ascension of the spacecraft relative to the tracking station when $t' = 0$. This allows tracking passes that are not symmetric about culmination to be represented by a simple rotation of the estimate covariance, which is much simpler algebraically than carrying a non-symmetric start and stop time for a tracking pass throughout the derivation. If q is redefined with an epoch in the middle of the non-symmetric pass, and a is redefined as \dot{r} in the center of the non-symmetric pass, then no further changes of variables are necessary. Consequently, the covariance for a symmetric pass will be obtained before any further considerations of asymmetry.

The partial derivatives matrix H of $\dot{\rho}$ with respect to a , b , c , and q for a series of measurements at times t_i is

$$H = \begin{pmatrix} 1 & \sin \omega t_1 & \cos \omega t_1 & t_1 \\ 1 & \sin \omega t_2 & \cos \omega t_2 & t_2 \\ \vdots & \vdots & \vdots & \vdots \end{pmatrix} \quad (4)$$

Using standard weighted least-squares formulation, the covariance P is

$$P = (H^T H)^{-1} \sigma_{\dot{\rho}}^2 \quad (5)$$

where $\sigma_{\dot{\rho}}^2$ is the variance of Doppler observations. The information array $\Lambda (= H^T H)$ is

$$\Lambda = \begin{pmatrix} N & \sum_j \sin \omega t_j & \sum_j \cos \omega t_j & \sum_j t_j \\ \sum_j \sin \omega t_j & \sum_j \sin^2 \omega t_j & \sum_j \sin \omega t_j \cos \omega t_j & \sum_j t_j \sin \omega t_j \\ \sum_j \cos \omega t_j & \sum_j \sin \omega t_j \cos \omega t_j & \sum_j \cos^2 \omega t_j & \sum_j t_j \cos \omega t_j \\ \sum_j t_j & \sum_j t_j \sin \omega t_j & \sum_j t_j \cos \omega t_j & \sum_j t_j^2 \end{pmatrix} \quad (6)$$

If the summation limits are symmetric with respect to the time origin (which is the time the spacecraft is at culmination) then all the odd functions will vanish. It is useful to introduce the following definitions:

$$\begin{aligned}
\psi &= \text{half-pass length in radians} \\
S &= \text{sampling interval (60 sec)} \\
N &= \text{number of points less 1} \\
&= \frac{2\psi}{S\omega}
\end{aligned}$$

It should be noted that in JPL navigation software the assumed accuracy of Doppler data is always referenced to a 60-second sample interval, making 60 seconds a convenient choice for S . The integral approximations of the summations in equation (6) can be expressed as

$$\begin{aligned}
\sum_j f(\omega t_j) &= \sum_{\omega t_j = -\psi}^{\omega t_j = \psi} f(\omega t_j) \\
&= \frac{N}{2\psi} \int_{-\psi}^{\psi} f(\varphi) d\varphi \\
&= \frac{1}{S\omega} \int_{-\psi}^{\psi} f(\varphi) d\varphi
\end{aligned} \tag{7}$$

Performing the integrals of the information array and replacing N with $2\psi/(S\omega)$, the following result is obtained:

$$\Lambda = \frac{1}{S\omega} \begin{pmatrix} 2\psi & 0 & 2\sin\psi & 0 \\ 0 & \psi - \frac{1}{2}\sin 2\psi & 0 & (2/\omega)(\sin\psi + \psi\cos\psi) \\ 2\sin\psi & 0 & \psi + \frac{1}{2}\sin 2\psi & 0 \\ 0 & (2/\omega)(\sin\psi + \psi\cos\psi) & 0 & (2\psi^3)/(3\omega^2) \end{pmatrix} \tag{8}$$

Note that $1/\omega$ shows up in the last column and row of Λ each time there is a factor of t_j that does not include ω .

Before inverting the information array, it is worth noting that the acceleration uncertainty often has some *a priori* information associated with it. If $\sigma_{q_{ap}}$ is the *a priori* uncertainty in the acceleration, then the last term of Λ is

$$\Lambda(4, 4) = (2\psi^3)/(3S\omega^3) + Q^2 \tag{9}$$

with

$$Q^2 = \frac{\sigma_{\dot{\rho}}^2}{\sigma_{q_{ap}}^2}$$

where $\sigma_{\dot{\rho}}$ appears due to the way the covariance will be defined. Typical values for $\sigma_{q_{ap}}$ are 10^{-12} km/sec², although for Ulysses the value is 2 orders of magnitude larger, as mentioned above. Assuming a typical (if conservative) measurement uncertainty of 1 mm/sec over a 60-second count time, the ratio Q^2 varies from 10^8 to 10^{12} for values of $\sigma_{q_{ap}}$ between 10^{-10} and 10^{-12} km/sec², which brackets the values of the first term of $\Lambda(4, 4)$. Consequently one may expect two sets of solutions depending of the value of $\sigma_{q_{ap}}$, with the solution for small $\sigma_{q_{ap}}$ being equivalent to the original Hamilton-Melbourne result with no acceleration term at all. For the some choices of Q , the result will depend equally on the both sets of solutions, but for most values one set will prevail.

The task of inverting Λ to get the covariance is made much easier by observing that Λ is really just two two-by-two matrices, as can be seen by reordering the parameters such that the state vector is $(a \ c \ b \ q)$. The inverse can then be obtained by inverting the two small matrices separately, giving the result

$$\sigma_a^2 = S\omega\sigma_\rho^2 \left[\frac{\psi + \frac{1}{2} \sin 2\psi}{2\psi^2 + \psi \sin 2\psi - 4 \sin^2 \psi} \right] \quad (10)$$

$$\sigma_{ac} = S\omega\sigma_\rho^2 \left[\frac{-2 \sin \psi}{2\psi^2 + \psi \sin 2\psi - 4 \sin^2 \psi} \right] \quad (11)$$

$$\sigma_c^2 = S\omega\sigma_\rho^2 \left[\frac{2\psi}{2\psi^2 + \psi \sin 2\psi - 4 \sin^2 \psi} \right] \quad (12)$$

$$\sigma_b^2 = S\omega\sigma_\rho^2 \left[\frac{\frac{2}{3}\psi^3 + Q^2 S\omega^3}{Q^2 S\omega^3 (\psi - \frac{1}{2} \sin 2\psi) - 2 \left(2\psi^2 - \frac{\psi^4}{3} + 2(1 - \psi^2) \sin^2 \psi + \left(\frac{\psi^3}{6} - 2\psi \right) \sin 2\psi \right)} \right] \quad (13)$$

$$\sigma_{bq} = S\omega^2\sigma_\rho^2 \left[\frac{-2(\sin \psi - \psi \cos \psi)}{Q^2 S\omega^3 (\psi - \frac{1}{2} \sin 2\psi) - 2 \left(2\psi^2 - \frac{\psi^4}{3} + 2(1 - \psi^2) \sin^2 \psi + \left(\frac{\psi^3}{6} - 2\psi \right) \sin 2\psi \right)} \right] \quad (14)$$

$$\sigma_q^2 = S\omega^3\sigma_\rho^2 \left[\frac{\psi - \frac{1}{2} \sin 2\psi}{Q^2 S\omega^3 (\psi - \frac{1}{2} \sin 2\psi) - 2 \left(2\psi^2 - \frac{\psi^4}{3} + 2(1 - \psi^2) \sin^2 \psi + \left(\frac{\psi^3}{6} - 2\psi \right) \sin 2\psi \right)} \right] \quad (15)$$

Equations 10-12 are identical (after some minor algebra) to comparable equations in Refs. 1 and 2. The complete independence of the uncertainty of a and c from the effects of adding an acceleration term is striking, although in retrospect it can be explained due to the orthogonality of the even functions 1 and $\cos \omega t$ with the odd functions $\sin \omega t$ and t . Equations 13-15 show the two families of solutions depending on the value of Q . The value of $S\omega^3$ is $2.33 \times 10^{-11} \text{ sec}^{-2}$, which requires Q^2 to be on the order of 10^{12} sec^2 (corresponding to $\sigma_{q_{ap}} = 10^{-12} \text{ km/sec}^2$) to dominate these equations. When Q^2 is sufficiently large, σ_b^2 approaches the form found in Refs 1 and 2, which is always smaller than σ_c^2 . Thus the effect of adding significant acceleration uncertainty to a symmetric pass is to change the identity of the best-determined angular parameter from b to c . This effect can be clearly seen in Figure 1, which plots the estimate uncertainty for each parameter (including b with and without an acceleration uncertainty) as a function of the pass half-width ψ .

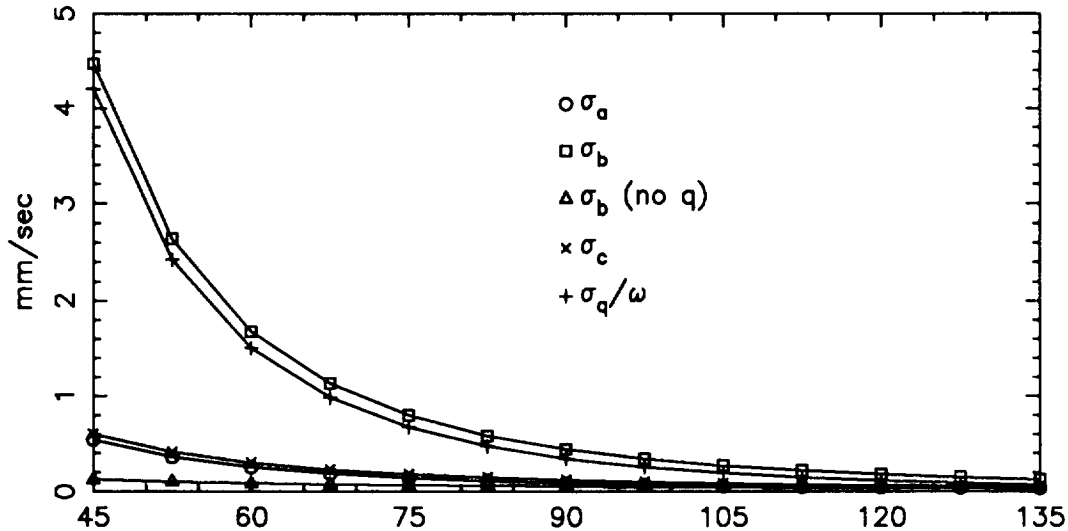


Figure 1: Parameter sigmas vs. pass half-width ψ (in degrees)

The two non-zero correlation coefficients are suggested by the close proximity of a to c and b to q/ω in Figure 1. The equations for the correlation coefficients are

$$\rho_{ac} = \frac{-2^{\frac{1}{2}} \sin \psi}{\psi(1 + \frac{1}{2\psi} \sin 2\psi)^{\frac{1}{2}}} \quad (16)$$

$$\rho_{bq} = \frac{-6^{\frac{1}{2}}(\sin \psi - \psi \cos \psi)}{\psi^2(1 - \frac{1}{2\psi} \sin 2\psi)^{\frac{1}{2}}} \quad (17)$$

assuming $Q^2 S \omega^3$ is small relative to other terms. As noted in Ref. 1, $-1.0 \leq \rho_{ac} \leq -0.9$ for pass lengths of 12 hours or less. However, tracking for 24 hours completely removes this correlation. On the other hand, $-1.0 \leq \rho_{bq} \leq -0.9$ for pass lengths of up to 20 hours, and $\rho_{bq} = -0.78$ for a 24-hour pass. This seems reasonable in consideration of the expansions of $(1 - \cos t)$ and $(t - \sin t)$ about zero, whose first non-zero terms are $t^2/2$ and $t^3/6$ respectively. If the geocentric angular velocity and acceleration of the a spacecraft was small enough that a 36 hour pass could be analyzed with these equations, ρ_{bq} would be -0.11 , but this is unlikely ever to be the case in practice. The values of ρ_{bq} and ρ_{ac} are plotted in Figure 2.

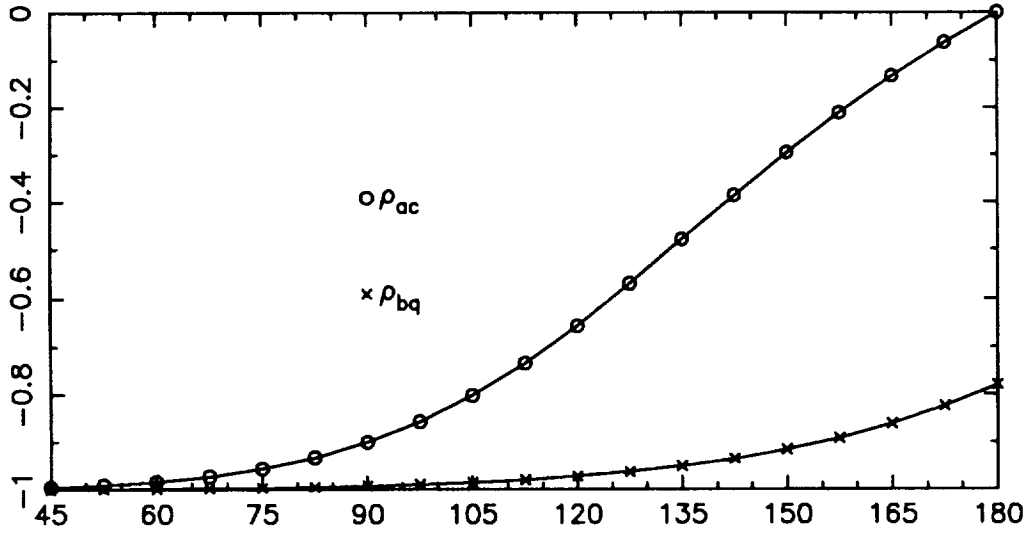


Figure 2: Correlation coefficients vs. pass half-width ψ (in degrees)

At this point it is useful to give the relationship between a , b , and c and r , α , and δ . At the time of Ref. 1, station location errors were a significant concern, but in the modern era, Very Long Baseline Interferometry (VLBI) measurements have reduced these errors to 10 cm or less 1σ , which largely remove their effect from estimates of the geocentric angular position of a spacecraft. Otherwise, the station longitude errors increase the right ascension uncertainty, and r_s errors increase both right ascension and declination uncertainty. It can be easily shown that

$$\sigma_r^2 = \sigma_a^2 \quad (18)$$

$$\sigma_\delta^2 \simeq \frac{\sigma_b^2}{(r_s \omega)^2 \sin^2 \delta} \quad (19)$$

$$\sigma_\alpha^2 \simeq \frac{\sigma_c^2}{(r_s \omega)^2 \cos^2 \delta} \quad (20)$$

$$\sigma_r^2 = \sigma_q^2 \quad (21)$$

by making use of the fact that ωt_0 is small (for Equation (20)). The usual navigation concern has been with declinations at or near zero, which causes a singularity in σ_δ for this approximation, although higher-order

terms and data arcs extending into regions of higher declination usually mitigate this effect in practice. A similar singularity would seem to exist at $\delta = 90^\circ$ for α , but this can be resolved by noting that the geocentric angular direction perpendicular to δ can be expressed $\alpha_n = \alpha \cos \delta$, so

$$\begin{aligned}\sigma_{\alpha_n}^2 &= \cos^2 \delta \sigma_\alpha^2 \\ &\simeq \frac{\sigma_c^2}{(r_s \omega)^2}\end{aligned}\tag{22}$$

again making use of the fact that ωt_0 is small. There is still a problem at exactly $\delta = 90^\circ$ because both b and c go to zero and cannot be separated. However, this situation is much less severe and more easily avoided than the problem that arises at zero declination.

The uncertainty predictions of these analytical results can now be evaluated using the Ulysses trajectory to produce high- and low-declination examples, which will later be checked against purely numerical results. On November 12, 1994, the declination of Ulysses was -75° , and the distance from the Earth was 330 million km. Neglecting the effects of acceleration uncertainty for the moment, and assuming a 24-hour pass (typical passes at the same station were over 6 days long), the following values are obtained:

$$\begin{aligned}\sigma_{\dot{r}} &= 0.0264 \text{ mm/sec} \\ \sigma_b &= 0.0373 \text{ mm/sec} \\ \sigma_\delta &\simeq 102 \text{ nrad} \\ \sigma_c &= 0.0373 \text{ mm/sec} \\ \sigma_\alpha &\simeq 380 \text{ nrad} \\ \sigma_{\alpha_n} &\simeq 98 \text{ nrad}\end{aligned}$$

The results above use 5205 km as a typical value of r_s for DSN stations. In terms of absolute position, the uncertainty is 32.4 km and 33.6 km in the direction of right ascension and declination, respectively, for an overall plane-of-sky position uncertainty of 46.7 km. If acceleration uncertainty with no *a priori* is included, the declination uncertainty increases to 163 nrad, or 53.6 km, for a total plane-of-sky position uncertainty of 62.6 km. Thus for very long passes at high declinations the effect of adding acceleration uncertainty is not severe.

In contrast, a 12 hour pass without acceleration uncertainty for a spacecraft with a declination of 10° would produce angular uncertainties of 324 nrad and 800 nrad for right ascension and declination, respectively. The large increase in the declination uncertainty is mostly due to the $(1/\sin \delta)$ term, as otherwise the declination uncertainty would be less than the right ascension uncertainty, due to the fact that $\sigma_c > \sigma_b$ when no acceleration is estimated. If acceleration uncertainty is included, the declination uncertainty increases to 6660 nrad, due to the large increase in σ_b . The addition of acceleration uncertainty therefore almost destroys any information about declination for spacecraft at fairly low declinations.

As mentioned earlier, the case of tracking passes that are not symmetric about the time of the spacecraft culmination may be handled by a rotation of the symmetric results. If ϕ is the offset of the center of the pass from the culmination point, then

$$\begin{pmatrix} c' \\ b' \end{pmatrix} = \begin{pmatrix} \cos \phi & -\sin \phi \\ \sin \phi & \cos \phi \end{pmatrix} \begin{pmatrix} c \\ b \end{pmatrix}\tag{23}$$

where b' and c' are the parameters b and c rotated by ϕ . The rotation matrix in equation (23) can be extended to be a full mapping matrix M , where

$$M = \begin{pmatrix} 1 & 0 & 0 & 0 \\ 0 & \cos \phi & -\sin \phi & 0 \\ 0 & \sin \phi & \cos \phi & 0 \\ 0 & 0 & 0 & 1 \end{pmatrix} \quad (24)$$

Then the covariance P' of $(a \ c' \ b' \ q)$ is given by

$$P' = M P M^T = \begin{pmatrix} \sigma_a^2 & \cos \phi \sigma_{ac} & \sin \phi \sigma_{ac} & 0 \\ \cos \phi \sigma_{ac} & \cos^2 \phi \sigma_c^2 + \sin^2 \phi \sigma_b^2 & \sin \phi \cos \phi (\sigma_c^2 - \sigma_b^2) & -\sin \phi \sigma_{bq} \\ \sin \phi \sigma_{ac} & \sin \phi \cos \phi (\sigma_c^2 - \sigma_b^2) & \cos^2 \phi \sigma_b^2 + \sin^2 \phi \sigma_c^2 & \cos \phi \sigma_{bq} \\ 0 & -\sin \phi \sigma_{bq} & \cos \phi \sigma_{bq} & \sigma_q^2 \end{pmatrix} \quad (25)$$

Equation (25) could be used to tailor the symmetry of the pass to obtain a better measurement of one angular direction at the expense of the other. However, the usefulness of these equations in the past would have been limited, because typical tracking passes for spacecraft in the ecliptic were over eight hours long anyway, and introducing asymmetry in the pass would have meant shortening the total tracking time, which is guaranteed to produce poorer results. In addition, the difficulty in measuring low values of declination means that a symmetric pass is generally the most desirable geometry in such cases.

This limitation does not apply to spacecraft at high declinations or to tracking schedules that have short pass lengths for programmatic reasons. In addition to Ulysses, an example of the first case would be NEAR after the Earth flyby, when the spacecraft is continuously in view for three months (longer than was the case for Ulysses) from the DSN complex at Canberra. Following the first 30 days after the flyby, NEAR requires only three 8-hour passes/week for telemetry purposes, as described in Reference 4. While NEAR navigation requires even fewer passes, Doppler data is expected from all telemetry passes, and so the 3 passes per week could be distributed to provide the same amount of information about both angular components. This can be accomplished by orienting the midpoints of the passes 6 hours (90°) apart. However, information about one component of the geocentric direction is often more important to navigation performance than information about the other component, which could lead to all the tracking being concentrated at one geometry. In the case of short pass lengths, such as the sparse four-hour passes typically proposed for Discovery missions during their cruise phases, the uncertainty in right ascension exceeds the uncertainty in declination for declinations over 8° . This might warrant specifying non-symmetric passes if right ascension information is important to the mission navigation.

While Ulysses is fairly unique in having a large acceleration uncertainty, such scenarios are possible on other spacecraft in contingency modes (which is actually the case for Ulysses as well). When the acceleration uncertainty exceeds about 10^{-11} km/sec², the declination uncertainty is maximized for a symmetric pass, so fixed-length tracking passes could be oriented in a non-symmetrical way to mitigate this effect. However, for spacecraft in the ecliptic, it is limited how much can be accomplished by this strategy, due to the half-day viewperiods and the additional uncertainty of media effects at low elevations, which degrade non-symmetric passes more than symmetric ones.

Another application of these equations is the use of one-way Doppler as a measurement, which is dependent on the stability of the spacecraft oscillator. (Two-way Doppler is also dependent on the stability of the reference oscillator at the tracking station, but the required stability is much more easily achieved on the ground than on a spacecraft). A parameter estimating a frequency rate on a spacecraft oscillator has the same form as an acceleration parameter, so \dot{f} could be substituted for q throughout these equations. As a frequency bias f_b is also typically present, $\sigma_a^2 = \sigma_r^2 + \sigma_{f_b}^2$, which limits the knowledge of geocentric range-rate to the *a priori* uncertainty of the frequency bias or a frequency bias estimate obtained over a several-month data arc.

Unfortunately, it must be noted that the estimation technique used for Ulysses operations, which involved eight independent accelerations per day, has not been successfully dealt with analytically. However, work

will continue in this area, because it should not require an inordinate amount of effort to develop this theory, especially with the existence of the results already presented here.

Numerical Results

The numerical results presented here were obtained using the JPL Orbit Determination Program, which includes both single-batch and batch-sequential least-squares modes. Both simulated and real tracking data with time spans ranging from 12 hours to two months were used to obtain the estimate covariances and orbit solutions discussed here.

In order to test the accuracy and relevance of the analytical results presented so far, the examples given above were simulated using the reconstructed Ulysses trajectory. On November 12, 1994, which at -75° is close to the maximum declination encountered in the southern pass, a total of 144 Doppler points with a 600 second sample time were simulated over 24 hours centered on spacecraft culmination. Only the geocentric angular position and range-rate were estimated to keep the filter from trying to estimate parameters that are only very poorly determined from one day of tracking, and no acceleration term was initially included. The resulting plane-of-sky uncertainty in the declination and right ascension directions was 54.0 km and 32.8 km, respectively. The right ascension uncertainty is almost exactly the same as the theoretical result presented earlier, while the declination result is 60 per cent higher. When a single radial acceleration is included with an *a priori* uncertainty of 10^{-10} km/sec² the results are 54.7 km and 33.2 km, which is very close to the predicted values, and the acceleration uncertainty was reduced to 1.1×10^{-12} km/sec², which is actually 35 per cent smaller than the predicted value. In each case, the radial velocity uncertainty was 5 mm/sec, which is about 200 times larger than the prediction. In both of these cases the numerically-computed correlation between the radial velocity and the right ascension is almost one, while the analytical correlation is zero. While this explains the larger radial velocity at one level, it is not clear why the correlation does not behave as predicted. Fortunately, the angular uncertainties are of primary interest, and the radial velocity uncertainty is still much better determined than any other velocity component.

The low declination case was examined using a 12 hour pass centered around culmination of the reconstructed Ulysses trajectory on December 10, 1992. In the absence of acceleration uncertainty, the plane-of-sky uncertainty in the declination and right ascension directions was 947 nrad and 363 nrad, respectively, which is about 15 per cent higher than predicted above. However, when acceleration was estimated, the plane-of-sky uncertainties were 6640 nrad and 446 nrad, respectively, and the acceleration uncertainty was 2.45×10^{-11} km/sec². The declination uncertainty is almost exactly as predicted, but the right ascension and acceleration uncertainty are about 40 per cent higher. The radial velocity uncertainty varies from 16 mm/sec without acceleration uncertainty, which is about 200 times larger than predicted, to 108 mm/sec with acceleration uncertainty. In contrast to the results above, the numerically-computed correlation between declination and radial velocity is almost -1 for both these cases, and the correlation between radial velocity and right ascension is about -0.6 . The declination and acceleration are highly correlated, as expected, so the radial velocity uncertainty increases with the declination uncertainty when acceleration is added to the filter. However, the reason for the high correlation between declination and radial velocity is not explained, nor is the difference between the radial velocity correlations for these two examples. It may be that the direction and magnitude of the angular rate of the spacecraft, and/or the radial acceleration of the spacecraft, play a greater role than expected. Fortunately, the angular uncertainties behave as expected for both of these cases, so the analytic results can still be used as an approximation of the angular information content of a pass of Doppler data.

The actual strategy used by Ulysses was evaluated using the high declination case ($\delta = -75^\circ$) by adding eight accelerations, each active over a three hour period and with an *a priori* uncertainty of 10^{-10} km/sec², which resulted in plane-of-sky uncertainties of 531 km and 535 km for the declination and right ascension directions, and a radial velocity uncertainty of 83 mm/sec. This roughly corresponds to the result of combining eight 4-hour passes, so it appears that while there is some continuity of angular information between acceleration intervals, the acceleration uncertainty at this level is enough to almost separate the estimates.

The result of extending one day data arcs to sixty to a hundred days is highly dependent on the trajectory of the spacecraft being tracked. The Ulysses trajectory is inclined almost 80° to the ecliptic, and the spacecraft velocity during the Southern pass is high due to its proximity to perihelion, which occurred in March, 1995. All of this contributes to a significant geometry change over any time span of two months or more during

the Southern pass, which helps to determine all of the components of the spacecraft state by mapping the observable quantities at one time into non-observable quantities at different epoch.

These long-arc effects are demonstrated on a time span extending one month on either side of November 12, 1994. During this time the spacecraft declination varied between -63° and -75° , and the spacecraft was continuously in view from the Canberra complex of the DSN. A total of 7790 usable Doppler points at 10 minute intervals were obtained during this time. There were seven attitude thruster events big enough to warrant separate treatment as impulsive delta-Vs as well. The estimated parameters included spacecraft state, solar pressure coefficient, one component of each impulsive maneuver, and a radial acceleration for each three-hour interval. The effects of the following consider parameters were also included: station locations, Earth ephemeris, and media calibrations. The filter parameters and Ulysses operational orbit determination techniques are described in much more detail in Reference 5, and will not be repeated here.

Solutions were obtained in this manner for a nominal *a priori* acceleration uncertainty of 10^{-10} km/sec², which was used operationally, and an alternate smaller *a priori* uncertainty of 10^{-11} km/sec². In both cases the smoothed covariance was mapped to the plane-of-the sky in the midpoint of the data arc. The nominal case produced an uncertainty of 74 km and 71 km in the declination and right ascension directions, and a range and range-rate uncertainty of only 42 km and 11 mm/sec. Since the geocentric range at this time is close to the heliocentric range, the primary effect determining the geocentric range is the heliocentric period of the spacecraft. Every parameter that can be compared with the similar one-day case above shows eight-fold improvement, which attests to the strength of the Earth-Sun-spacecraft geometry in determining the orbit based on such relatively poor one-day results.

While the nominal case had no consider parameters that made an appreciable difference in the results, the alternate case was strongly affected by the day-time component of the ionosphere. Before any non-estimated parameters were considered, the plane-of-sky uncertainties were 9 km in each component, while the range and range-rate uncertainties were 38 km and 1.4 mm/sec, respectively. After consider effects are applied, the plane-of-sky uncertainties were 19 km each, the range was unchanged, and the range-rate uncertainty was 2.5 mm/sec. These results show that the large *a priori* radial acceleration uncertainty increases the plane-of-sky uncertainty within the data arc, even though the radial uncertainty, based on the measurements over the entire data arc, is unchanged. It should also be noted that the Doppler data do not fit well at all for the alternate case, whereas the nominal case easily produces post-fit residual rms values of 0.13 mm/sec, well below the 1 mm/sec data weight. The nominal case also demonstrates that operational Ulysses solutions have difficulty meeting the 1000 km reconstruction requirement when data arcs of two to three months were used.

Conclusions

The Ulysses orbit determination experience provided the impetus to re-examine the information content of a single pass of Doppler data. Extending previous derivations to 24-hour passes and high declinations was found to be possible without difficulty, and a radial acceleration term was added. The acceleration term was found to significantly degrade declination estimates for symmetric passes. A simple means was developed to rotate the results of a symmetric pass to any other tracking geometry. While the agreement of the analytical results with numerical results leaves something to be desired in radial velocity, the analytical results are a useful predictor of angular and acceleration accuracy. The long-arc results show that the relative motion of the Earth and the spacecraft in their orbits around the Sun produces a much better result than could be obtained from a short-arc estimate.

Acknowledgements

This work was carried out at the Jet Propulsion Laboratory, California Institute of Technology, Pasadena, California, under contract with the National Aeronautics and Space Administration. The algebraic manipulator used here was the FAME package developed by Alex Konopliv. The detailed derivations of Muellershoen in Reference 2 were most helpful in understanding and extending previous work in this area. The authors would like to thank Jordan Ellis for the many helpful insights shared by him during discussions related to this paper.

References:

1. Hamilton, T. W., and Melbourne, W., G. "Information Content of a Single Pass of Doppler Data from a Distant Spacecraft," *JPL Space Programs Summary 37-39*, Vol. 3, May 31, 1966.
2. Muellerschoen, R. J. "Information Content of a Single Non-Symmetric Pass of Doppler Data from a Distant Spacecraft," JPL Interoffice Memorandum 314.5-1029, July 1, 1986.
3. Bertotti, B., Ambrosini, R., Asmar, S. W., Brenkle, J. P., Comoretto, G., Giampieri, G., Iess, L., Messeri, A., Vecchio, R., Wahlquist, H. D. "Ulysses' Gravitational Wave Experiment Report on the First Opposition," pg. 32, Istituto di Fisica dello Spazio Interplanetario, Frascati, Italy, December 1991.
4. "NEAR Detailed Mission Requirements," pg. 2-3, Johns Hopkins University/ Applied Physics Laboratory Document, November 1994.
5. McElrath, T. P, Tucker, B., Criddle, K. E., Menon, P. R., Higa, E. S. "Ulysses Navigation at Jupiter Encounter," AIAA/AAS Astrodynamics Conference, AIAA 92-4524, 10-12 August 1992.

